INFLUENCE OF INTERFACIAL $MoSe_2$ LAYERS ON ns LASER SCRIBING OF Cu(In, Ga)Se_2 SOLAR CELLS

Kai Kaufmann[1], Martina Werner[2], Sina Swatek[2], Malte Köhler[2], Christian Hagendorf[2],
[1] Hochschule Anhalt, University of Applied Sciences, 06366 Köthen, Germany
[2] Fraunhofer Center for Silicon Photovoltaics CSP, 06120 Halle, Germany

ABSTRACT: In many thin film photovoltaic technologies laser structuring is a common method to achieve the required monolithical series connection between neighboring cells. For CIGS solar cells P2 and P3 laser scribing using ultra short laser pulses (ps, fs)[i] has also been proven to be suitable but it is still not used in industry production. In this work, it is shown that nanosecond infrared laser pulses (1064 nm, 8 ns) are capable of removing the CIGS/CdS/ZnO layers from the underlying Mo substrate utilizing an explosive ablation process. SEM micrographs show that the resulting scribe edges exhibit clean fracture edges and are free of molten material for a broad distribution of laser parameters. The Mo layer remains completely intact. However, the outcome of the laser process strongly depends on the Mo/CIGS interface properties, like the presence of $MoSe_2$ or oxide layers. In order to understand the dominating interface properties, the composition of the CIGS/Mo interface as well as the presence of interfacial layers are analyzed in detail using XPS surface scans and ToF-SIMS low energy depth profiling. In particular, $MoSe_2$ layers are analyzed in terms of thickness and crystal orientation using TEM. Based on results from a quantitative pull test method, we found that the CIGS/Mo adhesion is crucial for successful laser scribing. Finally, mechanical and compositional interface properties are discussed and a model for the laser ablation based on the thermo-mechanical behavior of the CIGS layer stack under short pulse laser illumination is proposed.
Keywords: CIGS, laser scribing, thin film, interface

1 INTRODUCTION

Currently, the efficiency record for Cu(Ga, In)Se_2 based thin film photovoltaics is 20.4% achieved by EMPA/Swiss. Besides improving the properties of buffer and window layers the optimization of the monolithical series connection has large potential for additional gain of efficiency. The reduction of the dead zone by the use of smaller structures for electrical interconnection is directly connected to a rise of active solar cell area. Actually, laser scribing of CIGS solar cells is performed mainly in laboratory processing. In industry mechanical scribing is still the dominating technology.

Different approaches of laser scribing of CIGS thin films include the use of short laser pulses in the range of ns or ultra-short pulses in the range of ps and fs range [ii, iii]. Ultra short pulses utilize cold ablation to minimize thermal induced damage. Pulses in the ns range instead lead to several defects like melting of CIGS and the formation of conductive structures which may shunt the solar cell[i].

Infrared laser irradiation instead is able to penetrate the CIGS layer because the band gap of the absorber material is slightly higher than the laser energy. It has been proven that the use of 1064 nm pulses might be suitable to achieve the successful preparation of P3 like structures [iv, v].

In this work, 1064 nm laser pulses with a pulse length of 8 ns are used for P3 scribing with the goal to obtain a P3 scribe without any molten CIGS at the edges. Material properties like the presence of a $MoSe_2$ layer and adhesive forces between the CIGS and the Mo are investigated and related to characteristics of the resulting scribe structures.

2 EXPERIMENTAL

For the experiments 4 different samples 1a, 1b, 2a, 2b were used. CIGS was deposited in a coevaporation process (sample 1a, 1b Marti Luther University Halle Wittenberg; sample 2a, 2b industrial process). The layer structure is glass/Mo/CIGS/CdS and ZnO.

Scribing of CIGS layers is performed with pulsed laser (8 ns) irradiation with a wavelength of 1064 nm utilizing an explosive ablation or lift-off process. Using shorter wavelengths leads to melting of the CIGS material on the surface due to the higher absorption coefficient for 532 nm and 355 nm irradiation. However, laser energy and spot size have been varied systematically in order to achieve ablation structures with fractured edges free of residual material. The scribes are investigated using optical microscopy and SEM.

For adhesion measurements a pull test [vi] is used. The samples were cut into small pieces of a size of approximately 10 x 10 mm². Metal cylinders with a diameter of 5 mm were glued on top and bottom (see Fig. 1). The pull test experiment was carried out with a Zwick Z005 instrument. During the test a force normal to the CIGS/Mo interface was applied. This force was increased till delamination took place. After this the delaminated area was measured to calculate the adhesion strength.

Interface characterization of the CIGS/Mo interface was done using TEM. For this a TEM lamella was prepared with FIB techniques and the thickness and the crystallographic orientation of the $MoSe_2$ layer was measured. In addition the surface of the delaminated Mo and CIGS layers were measured after the pull test with XPS using an Axis Ultra instrument by Kratos. For this purpose the CIGS was pulled off the Mo substrate directly before transfer into the XPS instrument.

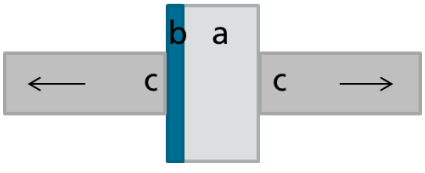

Fig. 1, Pull test schematically, a glass, b CIGS, c metal cylinders glued on the sample surface, the arrows indicate the applied forces.

3 RESULTS

3.1 Scribing results

On the sample group 1 (samples 1a, 1b) successful ablation was achieved using pulse energies in the range of 89 µJ to 120 µJ. **Fig. 2** shows the results. In this case a spot size of about 100 µm was used. The scribes are homogeneous without large variation in width. The best result was achieved with pulse energies of 104 µJ. **Fig. 3** shows two SEM micrographs of a scribe edge of a large diameter scribe of about 100 µm width. The Mo surface is free from residuals near the scribe edges. There are droplets of recrystallized material towards the center of the scribe. This leads to the conclusion that the ablated CIGS area is larger than the area in which melting of the CIGS occurs. The edge itself is free from molten material and provides clean cracks throughout the complete layer stack. The Mo surface is not damaged without traces, cracks or other visible structural defects.

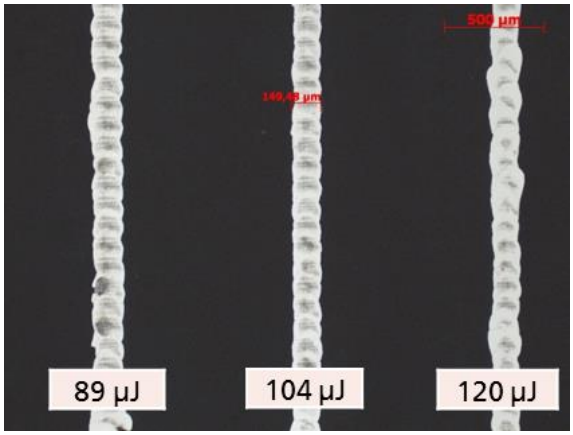

Fig. 2, Optical micrograph of successfully ablated P3 laser scribes for different pulse energies. Residuals are visible in the scribe center.

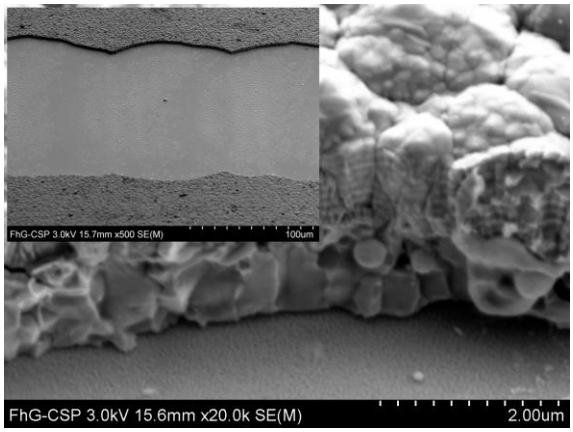

Fig. 3, SEM micrographs of the P3 scribe edge. The inset shows an overview of the scribe. The scribe edges and the bottom of the scribe nearby are free from molten CIGS or other residuals.

Reducing the spot size to less than 30 µm leads ultimately to a selective ablation of the ZnO which is shown in Fig. 4. At the bottom of the scribe the Mo layer is not visible. Instead the surface of molten and recrystallized CIGS is identified. Since reducing the spot size leads to an increase of the laser fluence, the ZnO delaminates from the underlying layer because of evaporating CIGS. The ZnO forms flat floe shaped pieces that are redeposited at the surrounding surface (not shown here).

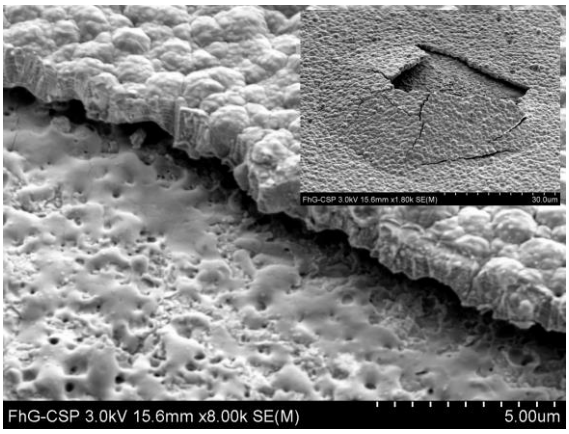

Fig. 4, At the inset, a SEM micrographs of a small laser ablation structure (diameter 5 µm) is shown. The high resolution image displays a detail of the scribe edge and bottom. ZnO is removed selectively. The CIGS surface is molten and recrystallized close to the scribe edge. Some ZnO delamination is visible at the edge.

On sample group 2 (samples 2a, 2b) no selective ablation of the CIGS/CdS/ZnO layer stack was possible. Scribing with large and small beam diameter caused no ablation of the layer stack. Molten CIGS remained on the Mo. ZnO was removed at small beam diameters of about 30µm.
Based on the scribing results the following three step model is proposed **Fig. 5**. In the first step (step a) heating up of the CIGS material causes thermal expansion and therefore tensile stress at the CIGS/MoSe2 interface. A delamination (step b) at the CIGS/MoSe2 occurs in the case of low adhesion. Due to the high fluence the CIGS melts and evaporates (step c) in the beam center. The delaminated CIGS is removed by an explosive lift-off mechanism.

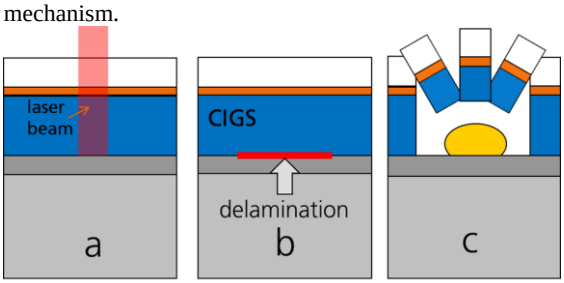

Fig. 5, Laser scribing process schematically, step a: heating of CIGS, step b: delamination, step c: explosive lift-off process with molten CIGS residual (yellow)

For successful scribing the delaminated area has to be larger in size than the molten area. Otherwise no removal of the whole CIGS/CdS/ZnO will occur. Since delamination of the CIGS from the Mo layer is required for forming clean scribes without molten CIGS the CIGS/Mo interface layer is investigated in greater detail.
The measured adhesion stress for a successful ablation

has to be below 10 N/mm².

3.2 Microstructural investigations

TEM investigations of the $MoSe_2$ layer of sample 2a (**Fig. 6**) show a 10 nm thick $MoSe_2$ layer. The c axis of the layer is orientatied pependicular to the interface plane. The distance between the single layers is 6.5 Å. This is in good agreement with values measured for hexagonal $MoSe_2$ [vii]. The $MoSe_2$ layer of sample 2b was about 50 nm thick. In this case the c axis is not oriented in a preferred normal or parallel direction to the interface (**Fig. 7**).
Since the $MoSe_2$ layers in sample 1a and 1b could not be clearly identified using TEM the thickness was estimated by ToF-SIMS depth profiles of the Mo layer after removal of the CIGS (not shown here). Assuming a constant sputter rate of the $MoSe_2$ for all of the four samples the thickness can be calculated from the depth profiles using the measured values from the TEM images of samples 2a and 2b. **Fig. 8** shows the thicknesses of all $MoSe_2$ layers ranging from 3 nm to 50 nm based on TEM calibrated TOFSIMS data.

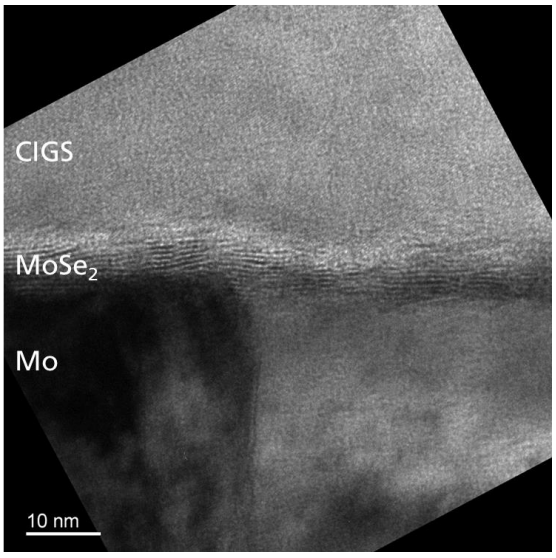

Fig. 6, TEM micrograph of MoSe2 layer of the sample 2a, the MoSe2 sheets are clearly visible. The orientation is mainly parallel to the Mo surface.

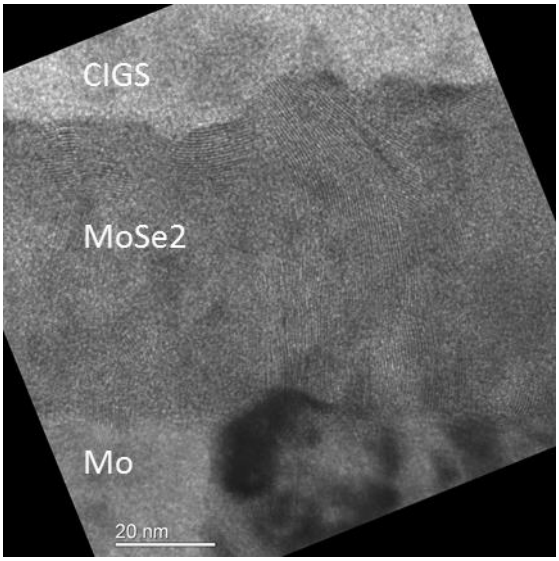

Fig. 7, TEM micrograph of $MoSe_2$ layer of the sample 2b, the $MoSe_2$ thickness is about 50 nm. The $MoSe_2$ sheets are not oriented in a preferred direction.

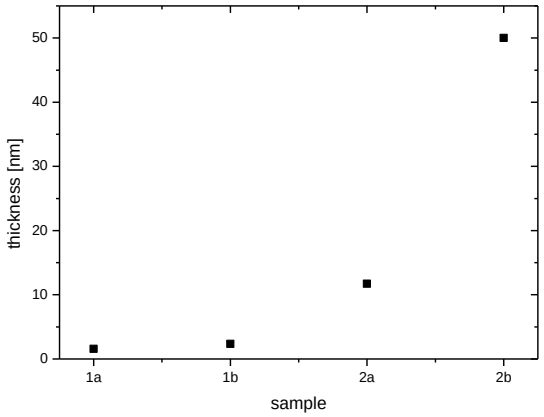

Fig. 8, thickness of the $MoSe_2$ layers, determined with TEM calibrated ToF-SIMS depth profiling (indicate the tolerances of the measurement).

3.3 Adhesion and composition

Using the pull test methode the adhesion stress was measured between theCIGS and the Mo layer. The experiment was repeated 8 times for each of the samples. The results show large differences between samples from group 1 (samples 1a, 1b) and from group 2 (sample 2a, 2b). Adhesion of group 2 was significantly higher than in group 1 (1a: 4.6 N/mm², 1b: 5.2 N/mm², 2a: 13.0 N/mm², 2b: 11.9 N/mm²). However, sample 2a shows a high variation for σ_V. Possible reasons are inhomogeneities at the CIGS/Mo interface.
However, the orientation and the thickness of the $MoSe_2$ of sample 2a and 2b were different Sample 2a showing a thin MoSe2 layer with the dense lattice parallel to the interface, wheras sample 2b exhibits a thick MoSe2 layer without any preferential lattice orientiation. Accordingly, it is assumed that MoSe2 thickness and crystal orientation is not the main reason for different adhesive forces of the CIGS/Mo interface.

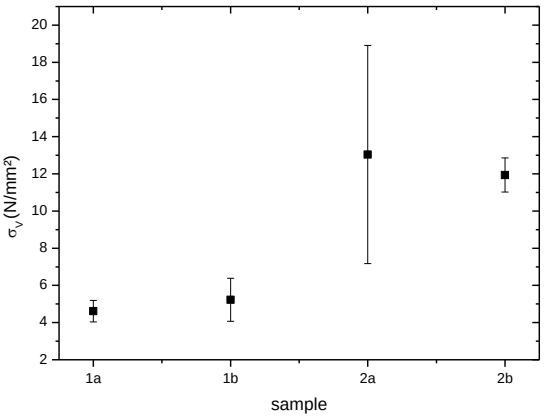

Fig. 9, Adhesive stress from pull test measurements with samples of group 1 (1a, 1b) showing reduced adhesive forces in comparison to samples of group 2 (2a, 2b).

Since the properties of the $MoSe_2$ layer could not be directly related to the observed adhesion properties, the question arises if the delamination is taking place within the $MoSe_2$ layer or rather at the Mo/$MoSe_2$ or at the $MoSe_2$/CIGS interfaces. In order to locate the position of the delamination crack as well as the composition of the Mo/CIGS interfacial layers the delaminated sample surfaces have been investigated using XPS after pull tests. XPS surface spectra of both the Mo and the CIGS surface after delamination are aquired.

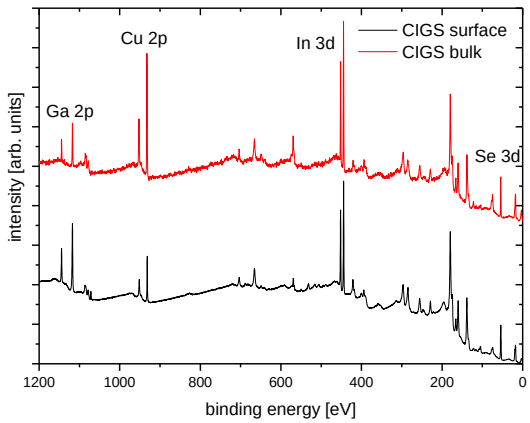

Fig. 10 Composition of the delaminated CIGS surface from the Mo/CIGS interface (black curve) in comparison to CIGS bulk material (red curve) as measured by XPS

Fig. 10 shows the surface composition of the delaminated sample 2b as measured by XPS in comparison to CIGS bulk material. The spectrum shows no Mo peaks (major peak expected at 227.5 eV). The XPS intensity distribution corresponds to that of the CIGS bulk material. Thus, no traces of an atom layer thick Mo coverage can be detected which indicates a complete delamination of the $MoSe_2$ layer. Similar results are obtained for the other samples.
XPS overview measurements of the delaminated Mo surfaces do not show any traces of Ga, Cu and In in the case of sample 2a and 2b. In sample 1a and 1b surface concentrations of Ga, Cu and In of less than 5% are found which may be due to local particles.

These results lead to the consistent conclusion that in all cases the delamination occurs directly at the CIGS/$MoSe_2$ interface. The structural and mechanical properties of the $MoSe_2$ layer are of less importance.

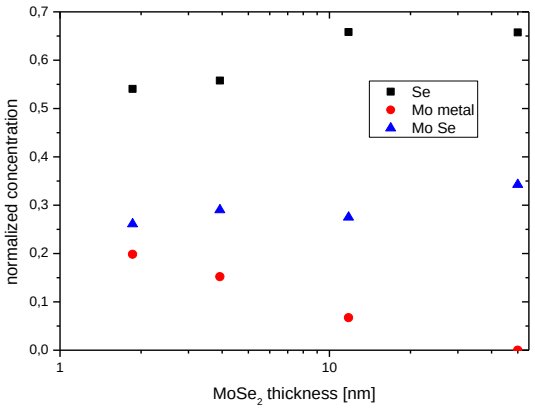

Fig. 11, Mo (metallic, Se coordination) and Se surface concentration the Mo surface for different $MoSe_2$ thicknesses. The Mo metal peak vanishes for thicker $MoSe_2$ layers, due to the limited information depth of XPS.

XPS investigations with high spectral resolution on delaminated Mo samples (not shown here) indicate that the Mo 3d 5/2 peak is composed of two components 227,89 eV 227,11 eV. The 227,11 eV peak corresponds to metallic Mo, the 227,89 eV peak to Mo in Se coordination. The 227,89 eV peak is shifted 0.8 eV towards higher binding energies.

In **Fig. 11** the surface concentration of the peak components of Mo (metallic, Se coordination) and Se are plotted as a function of the $MoSe_2$ thickness as obtained from the samples 1a, 1b, 2a, 2b. The intensity of the metallic Mo peak decreases with increasing $MoSe_2$ layer thickness. The Mo (Se coordination) and the Se peaks are slightly increasing with $MoSe_2$ thickness. This supports the assumption that the $Mose_2$ layers with different thickness remain completely on the Mo surface.

In addition to various previous investigations [viii, ix] we conclude the properties of the $MoSe_2$ layer like thickness and the crystal orientation are not the dominating factors for CIGS/Mo adhesion. In contrast, we have shown that delamination/ablation is occuring in general at the $MoSe_2$/CIGS interface. This interface is the mechanically weakest part of the layer stack. However, microstructure and elemental composition (Na, O) of the interface and residual stresses of the Mo or the CIGS layer are known to be an important factor for adhesion strength [x].

5 CONCLUSIONS

Successful laser scribing was achieved on samples with low CIGS adhesion for pulse energies 90 µJ to 120 µJ. A pull test setup was used to measure the adhesion quantitatively: delamination/laser ablation of CIGS from the Mo may be performed for $\sigma_V < 10$ N/mm². Systematic TEM and TOFSIMS investigations of the thickness and

crystal orientation show that these $MoSe_2$ properties like thickness and orientation are not crucial for the ns ablation.
In contrast, XPS measurements show that the delamination occurs exclusively at the CIGS/$MoSe_2$ interface. The structural, chemical and mechanical properties of this interface are determining the adhesive forces and therefore the feasibility of ns laser scribing.

6 ACKNOWLEDGEMENTS

This work was carried out within the joint research graduate school ''StrukturSolar'' of Anhalt University of Applied Sciences and Martin-Luther-University Halle-Wittenberg which is funded by the German Ministry of Education and Research under identification code 03SF0417A and SPAC number. Also financial support by the BMBF (Wachstumskern S-PAC Verbundprojekt 05, 03WKBW05C) is gratefully acknowledged.

[i] D Ruthe, K Zimmer and T Höche, Etching of $CuInSe_2$ thin films, comparison of femtosecond and picosecond laser ablation, Applied surface science, 2005, 247, 447—452

[ii] Raciukaitis, G. & Gecys, P, Picosecond - Laser Structuring of Thin Films for CIGS Solar Cells, Proceedings of LAMP2009 - the 5th International Congress on Laser Advanced Materials Processing, 2009

[iii] P. Gecys, G. Raciukaitis, M. Ehrhardt, K. Zimmer, & Gedvilas, ps-laser scribing of CIGS films at different wavelengths, Applied Physics A: Materials Science & Processing, Springer Berlin / Heidelberg, 2010, 101, 373-378

[iv] R. Murison, C. Dunsky, M. Rekow, C. Dinkel, J. Pern, L. Mansfield, T. Panarello & S. Nikumb, CIGS P1, P2, P3 Laser Scribing with an Innovative Fiber Laser, Photovoltaic Specialists Conference (PVSC), 2010 35th IEEE, 2010

[v] Buzás, A. & Geretovszky, Z., Nanosecond laser-induced selective removal of the active layer of CuInGaSe2 solar cells by stress-assisted ablation, Physical Review B, APS, 2012, 85, 245304

[vi] TR Hull, JS Colligon, AE Hill, Measurement of thin film adhesion, Vacuum, Volume 37, Issues 3–4, 1987, Pages 327-330

[vii] Agarwal, M. K., and L. T. Talele. Growth conditions and structural characterization of molybdenum sulphoselenide single crystals: (MoS_xSe_{2-x}, $0 \leqq x \leqq 2$). Materials Research Bulletin 20.3 (1985): 329-336.

[viii] Abou-Ras, D., et al. Formation and characterization of $MoSe_2$ for Cu (In, Ga)Se_2 based solar cells. Thin Solid Films 480 (2005): 433-438.

[ix] R. Würz, D. Fuertes Marrón, A. Meeder, A. Rumberg, S.M. Babu, Th. Schedel-Niedrig, U. Bloeck, P. Schubert-Bischoff, M.Ch. Lux-Steiner, Thin Solid Films, 431–432 (2003), p. 398

[x] Wiedeman, S., et al. CIGS module development on flexible substrates, Photovoltaic Specialists Conference, 2002, Conference Record of the Twenty-Ninth IEEE. IEEE, 2002